A&A 419, 241–247 (2004)
DOI: 10.1051/0004-6361:20035931

Astronomy & Astrophysics

Research Note

Discovery of [FeII]- and H_2-emission from protostellar jets in the CB3 and CB230 globules

F. Massi[1], C. Codella[2], and J. Brand[3]

[1] Osservatorio Astrofisico di Arcetri, INAF, Largo E. Fermi 5, 50125 Firenze, Italy
[2] Istituto di Radioastronomia, CNR, Sezione di Firenze, Largo E. Fermi 5, 50125 Firenze, Italy
[3] Istituto di Radioastronomia, CNR, via P. Gobetti 101, 40129 Bologna, Italy

Received 22 December 2003 / Accepted 2 March 2004

Abstract. Four Bok globules were studied in the Near-Infrared, through narrow-band filters, centered at the 1.644 μm line of [FeII], the H_2-line at 2.122 μm, and the adjacent continuum.
We report the discovery of [FeII] and H_2 protostellar jets and knots in the globules CB3 and CB230. The [FeII]-jet in CB230 is defined by a continuous elongated emission feature, superimposed on which two knots are seen; the brighter one lies at the tip of the jet. The jet is oriented in the same direction as the large-scale CO outflow, and emerges from the nebulosity in which a Young Stellar Object is embedded. The H_2 emission associated with this jet is fainter and wider than the [FeII] emission, and is likely coming from the walls of the jet-channel.
In CB3 four H_2 emission knots are found, all towards the blue-shifted lobe of the large-scale outflow. There is a good correspondence between the location of the knots and the blue-shifted SiO(5−4) emission, confirming that SiO emission is tracing the jet-like flow rather well. No line emission is found in the other two targets, CB188 and CB205, although in CB205 faint line emission may have been hidden in the diffuse nebulosity near the IRAS position. Around this position a small group of (≥10) stars is found, embedded in the nebula. A diffuse jet-like feature near this group, previously reported in the literature, has been resolved into individual stars.

Key words. stars: formation – ISM: jets and outflows – infrared: ISM

1. Introduction

Outflow and infall are inextricably associated with the very earliest stages of star formation. Even while still accreting matter, a newborn star generates a fast, well-collimated stellar wind that forms jets which sweep up the ambient molecular gas, creating bipolar molecular outflows. The high-velocity winds create shocks, which heat the gas to thousands of K when breaking up into the ambient gas. Understanding the details of the mechanism producing the acceleration of the outflow is fundamental to the understanding of the star formation process itself.

Emission of millimetre molecular lines (usually CO) at excitation temperatures $T_{ex} \approx 10-20$ K, is used to study the outflow's large-scale morphology. Whereas this component consists mostly of swept-up cloud material, and as such offers a time-averaged picture, the *present* flow activity is represented by a fast, hot component, traced by H_2 ro-vibrational lines at $T_{ex} \sim 2000$ K. Where this jet-like component interacts with the slower flowing gas or the ambient cloud, bow-shaped shock fronts are visible. This component, at $T_{ex} \sim 100$ K, can be traced by mm-emission of molecular species that are produced only in a shock-driven chemistry (e.g. Bachiller 1996).

The link between the 10–100 K gas and the hot jet-component is not well understood. In particular, it is still an open question how the efficiency of the processes leading to chemical anomalies depends on the shock-type (J/C) and -characteristics. The comparison between the shocked gas components at different temperatures is thus fundamental to the study of the jet/outflow system and the energetics of the star forming process.

A very good place to study the jet-component, the large-scale outflow, and their interaction are the Bok globules: cold (10 K) and relatively isolated molecular clouds associated with star formation. A catalogue of such objects (at $\delta > -30°$) was compiled by Clemens & Barvainis (1988; hereafter CB). Because of their relatively simple structure, globules form mainly low-mass stars in small numbers, and are therefore without the observational confusion that one encounters in regions like Orion or Ophiuchus.

Send offprint requests to: F. Massi,
e-mail: fmassi@arcetri.astro.it

Table 1. Centered coordinates of the observed globules.

Globule	α (J2000)			δ		
	h	m	s	°	′	″
CB3	00	28	42.3	+56	42	06.9
CB188	19	20	16.1	+11	35	57.0
CB205	19	45	24.1	+27	51	21.8
CB230	21	17	39.9	+68	17	31.9

With the italian TNG (Telescopio Nazionale Galileo) we have searched in four globules for the jet-component in the Near-InfraRed (NIR) through narrow-band H_2 (2.122 μm) and [FeII] (1.644 μm) filters. These two lines are particularly useful, as [FeII] traces (J-) shocks with velocities of a few 100 km s^{-1} and is therefore expected to outline the inner jet-channel, closest to the driving source of the flow. Molecular hydrogen, which dissociates at shock velocities >25−45 km s^{-1}, traces slower (C-) shocks and is excited in bow shocks and in shock-wakes (e.g. Allen & Burton 1993) and is therefore a good probe for the region of interaction between jet and ambient material. All four globules have been observed in the broad-band NIR (Yun & Clemens 1994a) and detected at 1.3 mm continuum (Launhardt & Henning 1997) and were found to contain embedded objects. Molecular outflows were also found in all four objects (Yun & Clemens 1994b; Codella & Bachiller 1999). Together, these findings identify these globules as good candidates in a search for protostellar jets. In this paper we report the detection of H2 and [FeII] line emission knots and jets in two of the four globules.

2. Observations and data reduction

Observations were carried out with the 3.58-m Italian Telescopio Nazionale Galileo (TNG) on La Palma (Canary Islands, Spain) on July 13–14, 2002. The images were obtained with the Near Infrared Camera Spectrometer (NICS; Baffa et al. 2001) through narrow-band filters centered on the 1.644 μm [FeII] $a^4D_{7/2} - a^4F_{9/2}$ and 2.122 μm H_2 $v = 1-0$ S(1) lines and on the adjacent continuum at 1.57 μm ($H_{\rm cont}$) and 2.28 μm ($K_{\rm cont}$). NICS is based on a 1024 × 1024 HgCdTe Hawaii array detector; we used a scale of 0.″25 pixel^{-1}, resulting in a field-of-view of 4.′2 × 4.′2. The 4 fields to be imaged were centered at the coordinates listed in Table 1, taken from Yun & Clemens (1992, 1994b) and Codella & Bachiller (1999) in order to cover all or most of the area of the molecular outflows.

For each field, a set of 13 to 26 images per filter were taken on a dithered pattern with maximum offsets (from the centre) of 30″ both in declination and right ascension. Total on-source integration times are in the range 20–26 min (H_2 and $K_{\rm cont}$) and 20–40 min ([FeII] and $H_{\rm cont}$). Standard stars AS34-0, AS37-0 and AS40-0 (Hunt et al. 1998) were imaged through all filters on a 5 position dithered pattern with the star at the centre of the array and within each quadrant, using integration times of 3 to 22 s (depending on the filter and the star's brightness) per position. Dithered sky frames in all filters were acquired at dawn and sunset and used to construct differential flat fields.

Each frame was first corrected for cross-talk using the routine provided on the TNG web page (`http://www.tng.iac.es/`). Then, data reduction was done using standard IRAF tasks. The obtained frames were corrected for bad pixels (through median averaging of the adjacent pixels) and distorsion, and then flat-fielded. For each field and filter, the underlying background was subtracted from each image in the dithered pattern by using the median of the 6 frames nearest in time. The same was done for the standard stars, but using 4 frames for the background. The images were then shifted to overlap, and averaged. Absolute coordinates were obtained through astrometry on HST Guide Stars present in (or near) the NICS fields, as explained in Massi et al. (1999).

3. Results and discussion

3.1. Removing the continuum

Observations in the H_2 and [FeII] filters contain, apart from the emission in the lines themselves (if present) also a contribution from the K- (in the case of H_2) and H-continuum (in the case of [FeII]). Therefore in order to detect the line emission the continuum has to be subtracted. Because the central wavelength of the continuum filters is different from those of the line filters, a proper subtraction requires a careful scaling of the emission detected in the continuum filters. Field stars are used for this, because their emission is expected to be continuum only.

We have assumed that the wavelength-dependence of the emission in the NIR is proportional to λ^x. The value of the slope x is derived from a comparison of the flux of a number of field stars in the line- and continuum filters.

In CB188 and CB205, no jet-like features are detected after subtraction, whereas in CB3 and CB230 pure H_2 and [FeII] emission knots and protostellar jets have been clearly revealed.

Photometry of the line-emission knots has been performed on the subtracted images using the task `POLYPHOT` in IRAF, roughly including the emission down to a $\sim 1\sigma$ limit. The sensitivity limit (of integrated line flux) is $2-3 \times 10^{-16}$ erg cm^{-2} s^{-1} arcsec^{-1}, both in the H_2 and in the [FeII] images; the limiting flux increases towards regions of diffuse emission.

3.2. CB3

This globule is associated with different generations of star formation, as suggested by the presence of a NIR Young Stellar Object (YSO; Yun & Clemens 1995, 1994a), a 1.3 mm object (Launhardt & Henning 1997), and a sub-mm source (Huard et al. 2000). This globule also contains an IRAS point source (IRAS 00259+5625), which lies among these objects; its flux is probably derived (in part) from contributions by these various objects. A molecular outflow was detected by Yun & Clemens (1992, 1994b) in CO and mapped in various molecular lines by Codella & Bachiller (1999), who found that the outflow is centered at or very near the 1.3 mm source, which is 17.″4 W, 1″ S of the IRAS position.

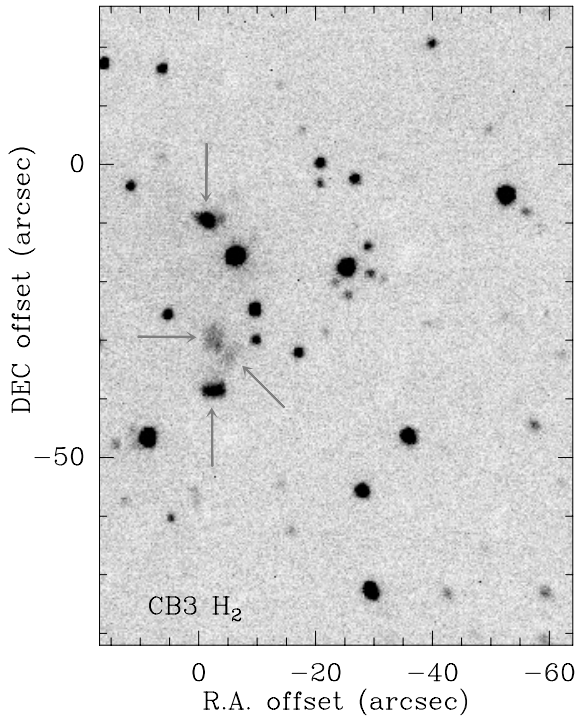

Fig. 1. TNG/NICS observations of CB3: the H_2 emission (still including the contribution from the continuum). The 4 knots (indicated by arrows) of H_2 line-emission are not at all visible in the K-continuum image (not shown).

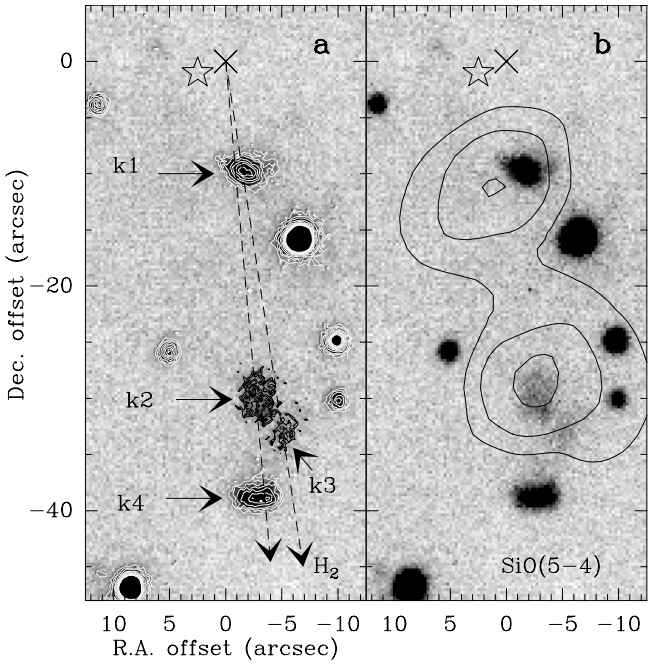

Fig. 2. a) A zoom-in on the four H_2 knots in CB3. To better outline k2 and k3, contours for them are drawn with smaller increments than for the other knots in the panel; lowest contour is at $\sim 2.5\sigma$. The dashed lines indicate the alignment of pairs of knots with the outflow centre. The centre of the outflow (Codella & Bachiller 1999) lies at offset (0, 0) and is indicated by a cross. The 1.3-mm peak (Launhardt & Henning 1997) is indicated by the star. **b)** As **a)**, but overlaid with the contours of integrated SiO(5–4) emission at $-42.5(\pm 0.5)$ km s^{-1} (Codella & Bachiller 1999). The angular resolution of the SiO map is 11″.

Our NIR images are centered on the centre position of the outflow. Figure 1 shows the image obtained in the H_2 filter. Even though this image still contains a contribution from the continuum, four regions of H_2 emission, hereafter called knots k1, k2, k3, and k4 (North to South), are clearly distinguishable; they are not present in the $K_{\rm cont}$-image (not shown). Figure 2a shows a close-up of the central region of the narrow-band line image; with the dashed lines we have tried to suggest how the spots can be aligned in pairs and how they may be traced back to the centre of the outflow (which, within the accuracy of the positions is presumably coincident with the 1.3 mm source). The lines show that the centers of k1 and k3 are aligned with the centre of the outflow, while the line connecting the origin of the flow and the centers of k2 and k4 is slightly offset from that. This may suggest a change of direction of the outflow axis with time.

Though unbeknownst to us at the time of the observations, the features k1 and k4 in Fig. 2a were already noted in deep NIR images of this region by Launhardt et al. (1998), who remarked that these two diffuse, non-stellar objects "might have H_2-line emission contributing to their K-band luminosity". The fact that these features are not visible in our $K_{\rm cont}$ image confirms that they arise from pure H_2 line emission. The absolute coordinates of the four H_2 knots, as well as their integrated flux, are given in Table 2.

Knot k4 lies at a distance of ∼40″ from the centre of the outflow; for an assumed distance of 2.5 kpc (Launhardt & Henning 1997) this corresponds to ∼0.5 pc. Knot k1 is the one nearest to the outflow centre, at a distance of 10″≈0.12 pc.

Table 2. List of coordinates and fluxes of the detected objects.

Object CB	α_{2000} ($^{\rm h}$ $^{\rm m}$ $^{\rm s}$)	δ_{2000} (° ′ ″)	$F_{\rm [FeII]}$ (erg cm^{-2} s^{-1})†	$F_{\rm H_2}$
3-k1	00 28 42.17	+56 41 57.36	<2.4−16	3.5−14
3-k2	00 28 42.12	+56 41 37.17	<2.4−16	1.4−14
3-k3	00 28 41.75	+56 41 34.20	<2.4−16	5.6−15
3-k4	00 28 42.12	+56 41 28.56	<2.4−16	2.1−14
205-A	19 45 24.15	+27 50 57.18	–	–
205-B	19 45 23.99	+27 50 59.25	–	–
230-A	21 17 38.36	+68 17 32.87	–	–
230-B1	21 17 40.09	+68 17 32.15	–	–
230-B2	21 17 39.96	+68 17 31.91	–	–
230-H_2	–	–	–	1.1−14
230-k1	21 17 38.11	+68 17 41.04	6.4−15	–
230-k2	21 17 38.12	+68 17 38.08	3.2−15	–

$\dagger$ $a-b$ means $a \times 10^{-b}$.

All knots are found South of the outflow centre, towards the blue lobe of the molecular outflow (Codella & Bachiller 1999). The fast outflow component is usually traced by H_2 line emission, which originates behind the shocks created where this jet-component interacts with the ambient cloud material. That we do not see any H_2 spots associated with the red (northern) lobe

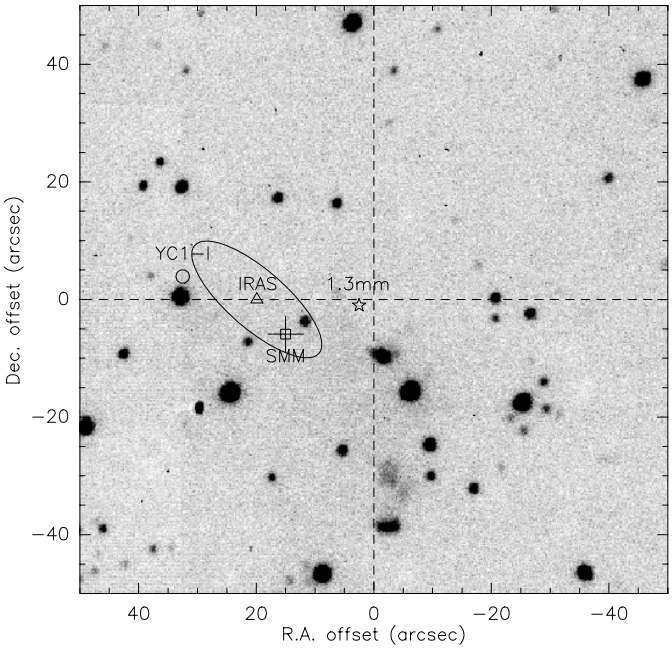

Fig. 3. CB3, H_2-band image (still including the contribution from the continuum). We have indicated the various signposts of star formation found associated with this globule: the NIR source YC1-I (Yun & Clemens 1995; circle), the IRAS point source (triangle), the 450 μm and 850 μm peaks (Huard et al. 2000; square), and the 1.3 mm source (Launhardt & Henning 1997; star). The centre of the outflow (Codella & Bachiller 1999) is at offset (0, 0).

of the outflow is likely because it is much more embedded in the globule, and the emission is too much obscured to be visible even at the NIR wavelength of H_2.

Closer inspection of the brightest knots k1 and k4 shows that the emission contours are slightly convex. Together with the knot alignment, and the location of the knots along the outflow axis, this argues in favour of the bow shock model for the interaction of a wind from the YSO and the ambient medium.

Downstream from the shocks caused by the interaction of the YSO-wind and the ambient medium, in high-density and -temperature gas, one expects to find an enhancement of several molecular species, which are liberated from the mantles of dust grains and injected into the gas phase through endothermic or gas-grain reactions as well as through sputtering. Codella & Bachiller (1999) have shown that the high-velocity component of the outflow in CB3 is well-traced by SiO, which is enhanced in the presence of shocks and which is only present along the main flow axis. In Fig. 2b we compare the location of the H_2 spots with channel maps of the (blue-shifted) emission of SiO(5–4). There is a close correspondence between the location of (at least two of) the H_2 spots and the peaks of the SiO distribution. This confirms that in CB3 the SiO emission is tracing the jet-like flow rather well, and indicates that along the outflow axis different temperature regimes coexist: the warm component at ~100 K (Codella & Bachiller 1999) traced by SiO and a hot (≥2000 K) component revealed by H_2.

In Fig. 3 we show the locations of the various tracers of star formation found in this globule, projected on the narrow-band H_2 image. An evolutionary sequence can be distinguished, in that we encounter progressively younger objects when going from the NIR-detected object YC1 (Yun & Clemens 1995), via the sub-mm peaks (Huard et al. 2000), to the 1.3 mm peak (Launhardt & Henning 1997), which is probably coincident with the centre of the outflow (Codella & Bachiller 1999). This implies that star formation in this globule has been going on for some time. Assuming the IRAS source and the sub-mm peaks refer to the same object, the mutual distance between the 3 star formation indicators in Fig. 3 is about 0.2 pc.

We take this opportunity to point out some inconsistencies in the original papers regarding the relative positions of the various objects plotted in Fig. 3. First, we note that the object identified as YSO (based on its NIR excess) in Yun & Clemens (1995) is different from the one they identified in CB3 in Yun & Clemens 1994a, which is about 100″ to the North. And even so, although YC1-I is a bright source (K = 8.24 mag; Yun & Clemens 1995), it does not coincide with any of the sources in our image – the nearest object (see Fig. 3) is ~4″ to the South, much more than the estimated positional accuracy (~2) of both our objects and YC1-I (~2″).

The relative positions of the Huard et al. (2000) sub-mm peak and the IRAS source are incorrect in their Fig. 1: based on the coordinates given by Huard et al. the sub-mm peak should be much closer to the IRAS position (~5″ rather than 15″). Although Launhardt & Henning (1997) do not give a positional accuracy for their 1.3 mm peak, it is probably similar to that of the sub-mm peak (i.e. ~3″), suggesting that these are different objects.

3.3. CB230

This globule also hosts a single IRAS source (IRAS 21169+6804), which is associated with the YSO found by Yun & Clemens (1994a). The YSO is located at the apex of a cone-shaped nebulosity (see Fig. 4) and is at the centre of a CO outflow (Yun & Clemens 1992; 1994b). The outflow is bipolar, but while the red component is quite compact, the blue lobe is more elongated, and extends northwards beyond the boundaries of the map made by Yun & Clemens (1994b) (i.e. its length >3′). Yun & Clemens (1994a) found a second NIR object, "possibly forming a binary system" together with the YSO at the base of the outflow. In our observations we find this second NIR object to consist of two nuclei, which would make this a triple system (Fig. 4). The conical nebula seen in Fig. 4 has a steep intensity-gradient towards the South, while towards the North the nebulous light fans out and decreases in intensity more gradually. The nebula opens up to the North, which is also the direction of the blue lobe of the outflow, the axis of which is North-South (Yun & Clemens 1994b). The approaching component of the bipolar outflow may have cleared out a cavity; the more extended emission seen in the northern part of the nebula could then be scattered light from walls of this cavity (see Yun & Clemens 1994a). Likewise, the diffuse emission associated with the embedded binary object ~9″ W of the main nebula is extended towards the SE (see Fig. 4). This might be the

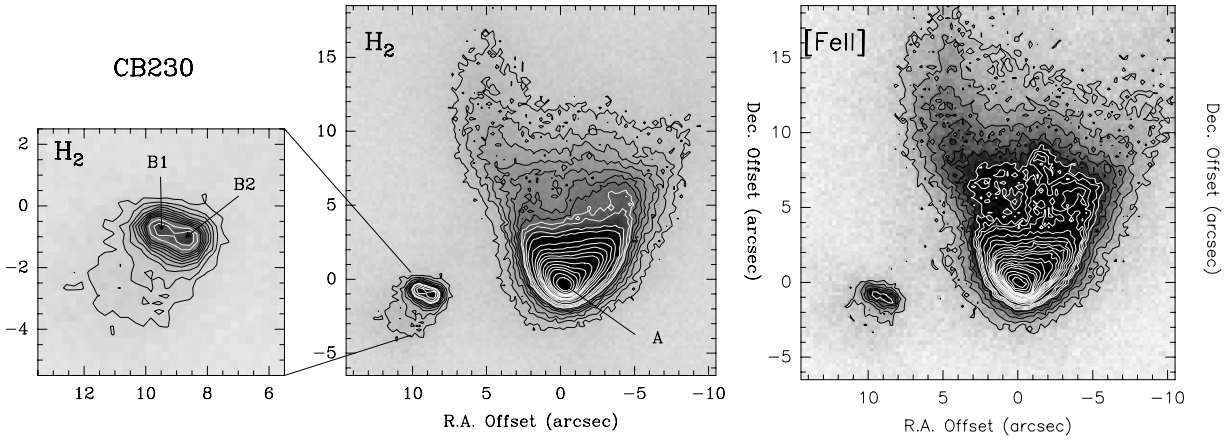

Fig. 4. Results of the TNG/NICS observations of CB230 of the H_2 and [FeII]-emission (still including continuum emission): (*central panel*) a zoom-in on the objects detected in H_2 in the core of CB230, with contours to better outline the more intense emission. The YSO is indicated by "A". (*Left*) A close-up of the smaller emission object, which is clearly seen to contain two sources (B1 and B2). The right-hand panel shows the contoured [FeII] emission (still including the continuum). A clear difference is seen in the diffuse emission just North of the YSO, with respect to the H_2 image (*central panel*); this is the signature of a jet (see Fig. 5).

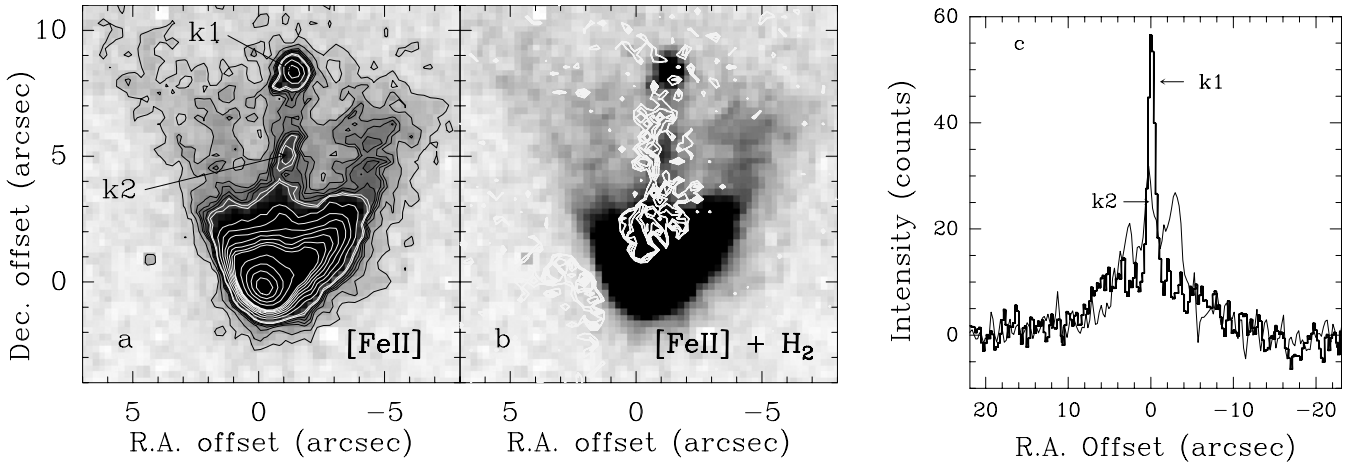

Fig. 5. A close-up of the jets and knots in CB230, after subtraction of the continuum. **a)** [FeII]-emission, and **b)** the same but overlaid with H_2 contours (white). **c)** Comparison of cuts through centre of the knots in the [FeII]-jet at constant Dec-offset from the continuum-subtracted image. The profile for knot k1 is drawn as a thick histogram, that for k2 as a thin line. Most of the elevated emission plateau between about −8″ and +9″ is an artifact of the mosaicing together of the different frames constituting the final image.

signature of an as yet undetected (or more likely: unresolved) outflow associated with the objects embedded herein.

Because we want to distinguish the (pure) line emission from the nebular emission, and because the spectral slope of the nebulosity differs from that of the field stars, we have determined the slope x of the wavelength dependence of the emission ($\propto\lambda^x$) by using the integrated flux of the northern part of the nebula, excluding the region with the embedded star. As we shall see (e.g. Fig. 5) the consequence of this is that in the continuum-subtracted [FeII]-image the YSO is still visible. Its spectral index differs from that of the nebula (which is radiation scattered by the dust), which we have used to scale the $H_{\rm cont}$-image; the YSO cannot therefore be correctly subtracted.

The final reduction, with careful scaling of the $H_{\rm cont}$- and $K_{\rm cont}$ images of the diffuse emission, reveals the pure line emission that remains after subtraction of the continuum, and is shown in Fig. 5: a jet is seen in [FeII], primarily defined by two knots along its length: a bright one at the tip (hereafter called k1) and a fainter one (k2) about half-way between k1 and the YSO. The knots are superimposed on a fainter, but clearly visible elongated emission feature. We stress that this detection is independent of potential inaccuracies in the continuum subtraction, as the knots are visible in the contours of the [FeII] image before continuum subtraction (cf. Fig. 4), but not at all in the ($H_{\rm cont}$) continuum image alone.

The jet is oriented in the N–S direction, and lies at the base of the large-scale molecular outflow. This jet is also traced by H_2 emission (Fig. 5b), which is weaker and slightly less narrow than that of [FeII]. Moreover, the H_2 emission appears to be anti-correlated with [FeII] peaking next to, rather than on the secondary knot in [FeII], and we conclude that in H_2 we probably see the *walls* of the jet-channel. The detection of strong [FeII]- and weaker H_2 emission suggests the presence of fast, dissociative J-shocks.

The total length of the jet, from its base at the location of the embedded YSO to the edge of knot k1 is about 9.″5,

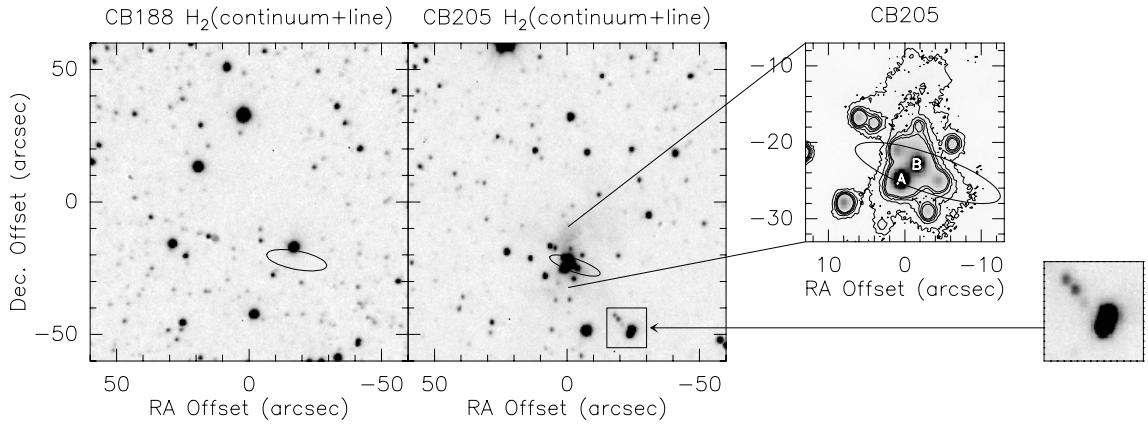

Fig. 6. Results of the TNG/NICS observations showing the H_2 emission, still including continuum emission, towards CB188 (*left panel*) and CB205 (*right panel*). The locations of the IRAS point sources are indicated by their uncertainty ellipses. The upper small panel on the far right shows a blow-up of the region around the IRAS source position in CB205. The lower small panel on the far right shows the alleged jet-like feature (Yun et al. 1993) being resolved into stars.

corresponding to ∼0.02 pc at the assumed distance of 450 pc (Launhardt & Henning 1997). Profiles of the knots in the [FeII]-jet, along cuts made at constant declination offsets and passing through the location of peak intensity of the knots, are shown in Fig. 5c. Both features are resolved in the NIR image. The width (*FWHM*) of k1 is 1.″2 corresponding to ∼540 AU. In the profile of k2 one can also identify the two intensity enhancements to the East and West, seen in Fig. 5a, which delineate the edges of the conical nebula. Both knots are superimposed on a broad (∼17″ ≈ 0.04 pc) plateau of emission; this is an artifact due to imperfect mosaicing, rendering the middle section of the image (in which the nebula and the jet are located) more noisy than the edges. The absolute coordinates of the three stellar objects (A, B1, and B2; Fig. 4) and of the two knots (k1, k2; Fig. 5a) in the [FeII]-jet are given in Table 2, where we also list the integrated fluxes of the two [FeII]-knots and the entire H_2 jet.

In addition to the main jet, a second [FeII]-feature is seen, emanating from the bright nebulosity and oriented in a N–NW-direction; this may indicate the existence of a second (unresolved) outflow, or it is a shock at the surface of the cavity, and thus related to the main jet.

3.4. CB188

In this globule, Launhardt & Henning (1997) detected 1.3 mm continuum emission, in the form of an "extended source with compact components" at the location of the IRAS source (indicated by the ellipse in Fig. 6). A YSO was detected at the same location by Yun & Clemens (1995), while Yun & Clemens (1994b) mapped a small (≤2′) outflow, of which the less extended blue lobe overlaps the red one.

Our continuum-subtracted H_2 and [FeII]-images do not show any line emission in the field down to the sensitivity limit. We also do not see the cometary diffuse emission around the possible NIR counterpart of the IRAS source that was found by Yun & Clemens (1994a; this would be the bright star seen just outside the IRAS error ellipse in Fig. 6), nor do we detect their source F, which they find embedded in this diffuse emission (see their Fig. 10b). It might be either a spurious detection or a variable object.

3.5. CB205

This globule, also known as L810, has an extended NIR nebulosity at the location of the IRAS source, as seen in Fig. 6. A NIR star cluster is associated with it; at least 10 stars can be seen within 10″ of the IRAS position (see the top-inset of Fig. 6).

The major axis of the nebula is oriented in a N–S direction, which is also the orientation of the compact molecular outflow detected by Yun & Clemens (1994b), of which the red and blue lobes show a significant overlap. This coincidence of orientations suggests a connection between the shape of the nebula and the presence of the outflow. However, no line emission has been found in our continuum-subtracted images, although we cannot rule out that some line emission knots may have been hidden in the more intense parts of the diffuse NIR nebulosity, near the IRAS point source location.

The nebula has been studied in the NIR (J, H, K) by Yun et al. (1993). The object they identified as the illuminator of the nebula, L810IRS, coincides with our star B in Fig. 6. Yun et al. (1993) also report the detection of an elongated jet-like feature, located about 35″ from L810IRS, to the SW. This feature is also visible in all our images (both line and continuum) and is seen to be resolved in a coincidental alignment of stars embedded in diffuse emission (see the lower-inset in Fig. 6, at $\Delta\alpha \sim -20''$ and $\Delta\delta \sim -45''$). No emission is left after continuum subtraction, further excluding a jet origin for it.

4. Summary

We have used NICS at the TNG to search for jet-components associated with molecular outflows in four globules, by imaging through narrow-band filters centered at [FeII] and H_2 and the adjacent continuum. Jets can be revealed, if present, after subtracting the scaled continuum emission from the image taken through the line filters. In two of our targets, CB3 and

CB230, this led to the identification of regions of pure line emission, while nothing was found in CB188 and CB205.

In CB3 we found four regions ("knots") of H_2 emission. All of these are located in the southern, blue lobe of the molecular outflow, which is probably driven by the 1.3 mm source located very near the centre of the outflow. There is a close correspondence between the location of the H_2-knots and the peaks in the SiO(5−4) emission (Codella & Bachiller 1999). The knots likely identify the locations where the jet-component of the outflow hits and shocks the ambient gas.

The relative locations of various signposts of star formation (embedded NIR source, IRAS point source, sub-mm and mm-peaks, and the outflow) suggest that star formation has been active for some time in this globule, and is progressing from East to West in CB3.

In CB230 we find a jet emerging from a conical nebulosity in which a YSO is embedded. The jet is oriented N–S, in the same direction as the large-scale molecular outflow. In the [FeII]-line the jet consists of two knots, the brighter one of which lies at its tip. Its length from the YSO at its base to its tip is about 0.02 pc (for d = 450 pc). The knots are superimposed on a substrate of lower-level diffuse emission. H_2 line emission is also detected, but this is fainter, and slightly wider than that of [FeII], suggesting that here we see the walls of the cavity in which the jet itself flows.

A second, fainter [FeII]-feature is seen to emerge from the nebulosity, and pointing in a NW-direction. This might either indicate the presence of a second, unresolved outflow, or be the locus of a shock at the surface of the cavity blown by the outflow.

About 9″ East of the YSO/nebula/jet-complex we find a smaller nebulosity containing two star-like nuclei. The nebulosity in which these are embedded has a steep intensity gradient to the NW, and shows a more gentle decrease towards the SE, analogous to what is seen in the main nebula. From the existing low-angular resolution CO maps it is not possible to tell if this binary object is associated with its own outflow.

Acknowledgements. The work presented here is based on observations made with the Italian Telescopio Nazionale Galileo (TNG) operated on the island of La Palma by the Centro Galileo Galilei of the INAF (Istituto Nazionale di Astrofisica) at the Spanish Observatorio del Roque de los Muchachos of the Instituto de Astrofisica de Canarias. A special thank you to Dino Fugazza and Gianni Tessicini for their help during the observations. We thank Rafael Bachiller for suggestions and stimulating discussions.

References

Allen, D. A., & Burton, M. G. 1993, Nature, 363, 54
Bachiller, R. 1996, ARA&A, 34, 111
Baffa, C., Comoretto, G., Gennari, S., et al. 2001, A&A, 378, 722
Clemens, D. P., & Barvainis, R. E. 1988, ApJS, 68, 257 [CB]
Codella, C., & Bachiller, R. 1999, A&A, 350, 659
Huard, T. L., Weintraub, D. A., & Sandell, G. 2000, A&A, 362, 635
Hunt, L. K., Mannucci, F., Testi, L., et al. 1998, AJ, 115, 2594
Launhardt, R., & Henning, Th. 1997, A&A, 326, 329
Launhardt, R., Henning, Th., & Klein, R. 1998, in Star formation with the Infrared Space Observatory (ISO), ed. J. L. Yun, & R. Liseau, ASP Conf. Ser., 132, 119
Massi, F., Giannini, T., Lorenzetti, D., et al. 1999, A&AS, 136, 471
Yun, J. L., & Clemens, D. P. 1992, ApJ, 385, L21
Yun, J. L., & Clemens, D. P. 1994a, AJ, 108, 612
Yun, J. L., & Clemens, D. P. 1994b, ApJS, 92, 145
Yun, J. L., & Clemens, D. P. 1995, AJ, 109, 742
Yun, J. L., Clemens, D. P., McCaughrean, M. J., & Rieke, M. 1993, ApJ, 408, L101